Ligand Design for Heterobimetallic Single-Chain Magnets: Synthesis, Crystal Structures, and Magnetic Properties of MIICuII (M=Mn, Co) Chains with Sterically Hindered Methyl-Substit...

ARTICLE *in* CHEMISTRY · FEBRUARY 2007

Impact Factor: 5.73 · DOI: 10.1002/chem.200600992 · Source: PubMed

9 AUTHORS, INCLUDING:

Emilio Pardo
University of Valencia
78 PUBLICATIONS **2,072** CITATIONS
SEE PROFILE

Juan Faus
University of Valencia
157 PUBLICATIONS **5,024** CITATIONS
SEE PROFILE

Yves Journaux
Pierre and Marie Curie University - Paris 6
158 PUBLICATIONS **5,024** CITATIONS
SEE PROFILE

Miguel A. Novak
Federal University of Rio de Janeiro
117 PUBLICATIONS **4,930** CITATIONS
SEE PROFILE

CHEMISTRY
A EUROPEAN JOURNAL

DOI: 10.1002/chem.200600992

Ligand Design for Heterobimetallic Single-Chain Magnets: Synthesis, Crystal Structures, and Magnetic Properties of $M^{II}Cu^{II}$ (M = Mn, Co) Chains with Sterically Hindered Methyl-Substituted Phenyloxamate Bridging Ligands

Emilio Pardo,[a] Rafael Ruiz-García,[b, f] Francesc Lloret,*[a] Juan Faus,[a] Miguel Julve,[a] Yves Journaux,[c] Miguel A. Novak,[d] Fernando S. Delgado,[e] and Catalina Ruiz-Pérez[e]

Abstract: Two new series of neutral oxamato-bridged heterobimetallic chains of general formula $[MCu(L^x)_2]\cdot m$DMSO (m = 0–4) (L^1 = *N*-2-methylphenyloxamate, M = Mn (**1a**) and Co (**1b**); L^2 = *N*-2,6-dimethylphenyloxamate, M = Mn (**2a**) and Co (**2b**); L^3 = *N*-2,4,6-trimethylphenyloxamate, M = Mn (**3a**) and Co (**3b**)) have been prepared by reaction between the corresponding anionic oxamatocopper(II) complexes $[Cu(L^x)_2]^{2-}$ with Mn^{2+} or Co^{2+} cations in DMSO. The crystal structures of $[CoCu(L^2)_2(H_2O)_2]$ (**2b′**) and $[CoCu(L^3)_2(H_2O)_2]\cdot 4H_2O$ (**3b′**) have been solved by single-crystal X-ray diffraction methods. Compounds **2b′** and **3b′** adopt zigzag and linear chain structures, respectively. The intrachain Cu···Co distance through the oxamate bridge is 5.296(1) Å in **2b′** and 5.301(2) Å in **3b′**, while the shortest interchain Co···Co distance is 5.995(5) Å in **2b′** and 8.702(3) Å in **3b′**, that is, the chains are well isolated in the crystal lattice due to the presence of the bulky methyl-substituted phenyl groups. Although both $Mn^{II}Cu^{II}$ and $Co^{II}Cu^{II}$ chains exhibit ferrimagnetic behaviour with moderately strong intrachain antiferromagnetic coupling ($-J_{Mn,Cu}$ = 24.7–27.9 cm^{-1} and $-J_{Co,Cu}$ = 35.0–45.8 cm^{-1}; $\mathbf{H} = \sum_i -J_{M,Cu}\mathbf{S}_{M,i}\mathbf{S}_{Cu,i}$), only the $Co^{II}Cu^{II}$ chains show slow magnetic relaxation at low temperatures (T_B < 3.5 K), which is characteristic of single-chain magnets (SCMs) because of the high magnetic anisotropy of the Co^{II} ion. The blocking temperatures T_B along this series of chains vary according to the steric hindrance of the aromatic substituent of the oxamate ligand in the series $L^1 < L^2 < L^3$. Analysis of the SCM behaviour for **3b** and **3b′** on the basis of Glauber's theory for a one-dimensional Ising system showed a thermally activated mechanism for the magnetic relaxation (Arrhenius law dependence). The activation energies E_a to reverse the magnetisation direction are 38.0 (**3b**) and 16.3 cm^{-1} (**3b′**), while the preexponential factors τ_0 are 2.3×10^{-11} (**3b**) and 4.0×10^{-9} s (**3b′**).

Keywords: cobalt · copper · magnetic properties · manganese · N,O ligands · supramolecular chemistry

Introduction

Magnetic chains have been actively investigated for the design and synthesis of molecular magnets, that is, molecule-based compounds exhibiting spontaneous magnetisation below a critical temperature T_C.[1,2] This novel molecular approach to magnetic materials consists of assembling ferrimagnetic heterospin chains in a ferromagnetic fashion with

[a] Dr. E. Pardo, Prof. Dr. F. Lloret, Prof. Dr. J. Faus, Prof. Dr. M. Julve
Departament de Química Inorgànica
Instituto de Ciencia Molecular, Facultat de Química
Universitat de València
Paterna, València, 46980 (Spain)
Fax: (+34) 96-354-4322
E-mail: francisco.lloret@uv.es

[b] Dr. R. Ruiz-García
Departament de Química Orgànica
Instituto de Ciencia Molecular, Facultat de Química
Universitat de València
Paterna, València, 46980 (Spain)

[c] Dr. Y. Journaux
Laboratoire de Chimie Inorganique et Matériaux Moleculaires
Université Pierre et Marie Curie–Paris6
UMR 7071, Paris, 75005 (France)

[d] Prof. M. A. Novak
Instituto de Física
Universidade Federal do Rio de Janeiro
Rio de Janeiro-RJ, 21945-970 (Brazil)

[e] Dr. F. S. Delgado, Prof. Dr. C. Ruiz-Pérez
Laboratorio de Rayox X y Materiales Moleculares
Departamento de Física Fundamental II
Facultad de Física, Universidad de La Laguna
Tenerife, 38204 (Spain)

[f] Dr. R. Ruiz-García
Fundació General de la Universitat de València
Universitat de València
València, 46002 (Spain)

Supporting information for this article is available on the WWW under http://www.chemeurj.org/ or from the author.

the possibility of achieving long-range three-dimensional (3D) magnetic order through interchain interactions.[3,4] Such an approach was first applied successfully by Kahn et al. in the oxamato-bridged manganese(II)–copper(II) chain $[MnCu(pbaOH)(H_2O)_3]$ (pbaOH = 2-hydroxy-1,3-propylenebis(oxamate); $T_C = 4.6$ K),[3a] and then extended to other heterobimetallic chains of the same family with varying results. For instance, the cobalt(II)–copper(II) chain analogue $[CoCu(pbaOH)(H_2O)_3]\cdot 2H_2O$ orders antiferromagnetically.[3b] Alternatively, Gatteschi et al. reported the manganese(II) nitronyl nitroxide chain $[Mn(hfac)_2(NITiPr)]$ (hfac = hexafluoroacetylacetonate, NITiPr = 2-isopropyl-4,4,5,5-tetramethylimidazolin-1-oxyl-3-oxide) as the first example of a metalloradical chain which orders ferromagnetically ($T_C = 7.6$ K).[4a] Despite the fact that the Cu^{II} ion ($S = 1/2$) had been replaced by a nitronyl nitroxide (NIT) radical ($S = 1/2$), a similar 1D ferrimagnetic behaviour was observed in the $Mn^{II}Cu^{II}$ bimetallic chains and the Mn^{II}NIT radical chains. The recent finding of slow magnetic relaxation and hysteresis effects in the cobalt(II) nitronyl nitroxide radical chain analogue $[Co(hfac)_2(NITPhOMe)]$ (NITPhOMe = 4′-methoxyphenyl-4,4,5,5-tetramethylimidazolin-1-oxyl-3-oxide),[5] which are not associated with 3D ordering but have a purely 1D origin, has renewed the field and opened exciting new perspectives for storing information in low-dimensional magnetic materials.[6]

As early as 1963, Glauber[7] predicted that a single chain with Ising-type magnetic anisotropy, either ferri- or ferromagnetic, should exhibit exponential divergence of the relaxation time τ of the magnetisation as the temperature decreases. This situation is reminiscent of that recently observed in some discrete polynuclear complexes, so-called single-molecule magnets (SMMs).[8a,b] These molecules have a large ground-state spin S and a large negative axial magnetic anisotropy D which result in a large activation energy E_a for the magnetisation reversal, given by $E_a = |D|S^2$. In the case of single chains, the activation energy depends on the intrachain coupling constant J according to the expression $E_a = (4|J| + |D|)S^2$.[8c] Although this theory has been known for more than forty years, it is only recently that the first example of a 1D compound exhibiting slow magnetic relaxation below a blocking temperature T_B, a so-called single-chain magnet (SCM), has been reported. An easy axis of magnetisation and a large ratio of intrachain to interchain coupling constants ($|J/j| > 10^4$) are both required to observe this unique magnetic behaviour experimentally. In spite of these restrictive requirements, some additional examples of SCMs were published in the last five years since the first example was reported by Gatteschi et al., which still exhibits the highest blocking temperature ($T_B \approx 15$ K).[5a] These include ferri- and ferromagnetic, homo- and heterobimetallic chains with different bridges and metal ions: 1) $[Mn_2(saltmen)_2Ni(pao)_2L_2](A)_2$ (saltmen = *N*,*N*′-(1,1,2,2-tetramethylene)bis(salicylideneiminate), pao = pyridine-2-aldoximate, L = N-donor monodentate ligand, and A = monoanion), which consists of chains of $Mn^{III}Ni^{II}Mn^{III}$ trinuclear units with alternating intratrimer antiferro- and intertrimer ferromagnetic interactions through oximato and phenolato bridges, respectively;[9] 2) $[\{FeL(CN)_4\}_2Co(H_2O)_2]\cdot n H_2O$ (L = 2,2′-bipyridine (bpy), 1,10-phenanthroline (phen) with $n = 4$, and L = 2,2′-bipyrimidine (bpym) with $n = 6$), which is made up of cyanide-bridged 4,2-ribbonlike chains with ferromagnetic coupling between the low-spin Fe^{III} and high-spin Co^{II} ions;[10a,c] 3) $[\{Fe(bpy)(CN)_4\}_2Co(H_2O)]\cdot MeCN\cdot 0.5H_2O$, which is a related cyanide-bridged double 4,2-ribbonlike chain with coexistence of intrachain ferro- and interchain antiferromagnetic interactions;[10b] 4) $[Co(bt)(N_3)_2]$ (bt = 2,2′-bithiazoline) which is composed of ferromagnetic azide-bridged helical chains of high-spin Co^{II} ions;[11] 5) $[\{Fe(Tp)(CN)_3\}_2Cu(CH_3OH)]\cdot 2CH_3OH$ (Tp = tris(pyrazolyl)borate), which consists of chains with ferromagnetic coupling between the high-spin Fe^{III} ions and the Cu^{II} ions;[12] and 6) $(NEt_4)[Mn_2(5\text{-MeOsalen})_2Fe(CN)_6]$ (5-MeOsalen = *N*,*N*′-ethylenebis(5-methoxysalicylideneiminate)), which consists of chains of $Mn^{III}Fe^{III}Mn^{III}$ trinuclear units with alternating intratrimer antiferro- and intertrimer ferromagnetic interactions through cyanide and phenolate bridges, respectively.[13]

Here we present a rational synthetic strategy to obtain SCMs which is based on the use of sterically hindered dianionic oxamatocopper(II) complexes as bis-bidentate ligands towards fully solvated, divalent transition metal cations such as manganese(II) and cobalt(II) (Scheme 1). This "complex-as-ligand" approach results in oxamato-bridged heterobimetallic chains with three different possible structures. The linear chain structure[14a,b] is obtained when the solvent molecules coordinate to the M^{II} ions (M = Mn and Co) in *trans* positions (Scheme 1a). When they coordinate in *cis* positions, zigzag[14c] or helical structures result, depending on the steric requirements of the Cu^{II} precursor complex (Scheme 1b and c, respectively).

We report the preparation and structural and magnetic characterisation of a novel series of heterobimetallic manganese(II)–copper(II) and cobalt(II)–copper(II) chains prepared from monomeric copper(II) complexes with the aromatically substituted oxamate ligands L^1 = *N*-2-methylphenyloxamate, L^2 = *N*-2,6-dimethylphenyloxamate and L^3 = *N*-2,4,6-trimethylphenyloxamate. In a preliminary communication,[15] we have shown that the combination of an orbitally degenerate octahedral high-spin Co^{II} ion ($^4T_{1g}$) and a square-planar Cu^{II} precursor with the L^3 ligand results in a large Ising-type magnetic anisotropy in the chain and minimisation of the interchain interactions. Both conditions were necessary to observe the phenomenon of slow relaxation of the magnetisation in the cobalt(II)–copper(II) chain $[CoCu(L^3)_2(H_2O)_2]\cdot 4H_2O$, where magnetic coupling between the Co^{II} and Cu^{II} ions through the oxamate bridge is large enough to allow long-range intrachain magnetic correlation ($-J = 35.0$ cm^{-1}).[15] At present, our goal is to perform a systematic analysis of the effect of the steric requirements in the Cu^{II} precursor complex (number of methyl substituents) and the local magnetic anisotropy of the M^{II} ion (M = Mn, Co) on the structure and magnetic properties of the resulting $M^{II}Cu^{II}$ chain compound. This work provides an example

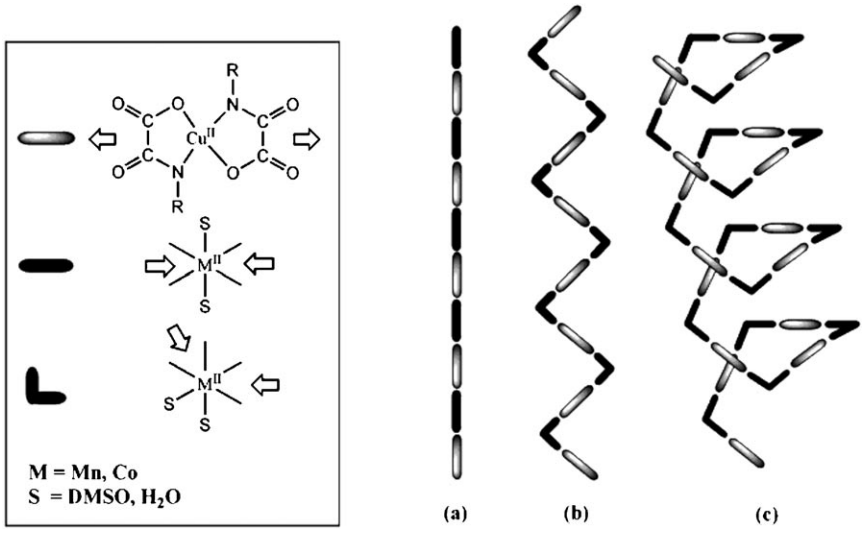

Scheme 1. Proposed structures for the oxamato-bridged heterobimetallic chain compounds: a) linear, b) zigzag and c) helical.

of successful design of a new family of oxamato-bridged heterobimetallic SCMs, which expand the range of the few reported examples of slowly magnetically relaxing 1D materials.

Results and Discussion

Synthesis and general physical characterization: Neutral oxamato-bridged $M^{II}Cu^{II}$ chains (M = Mn, Co) were synthesised in three successive steps (Scheme 2). The first is the synthesis of the *N*-substituted monooxamate ligands H_2L^x by straightforward condensation of ethyl chlorooxoacetate with three different aniline derivatives in THF (Scheme 2a). They were isolated as the ethyl ester derivatives $HEtL^x$ in excellent yields (ca. 80–100%). The second step consists of synthesising the mononuclear copper(II)–L^x complexes as their sodium salts of general formula $[Na_2Cu(L^x)_2]\cdot n H_2O$ (Scheme 2b). They were obtained in good yields (ca. 75–80%) by deprotonation and hydrolysis of the corresponding ligand $HEtL^x$ with NaOH in water, and subsequent addition of the stoichiometric amount of Cu^{II} as a nitrate salt. In the third step, the heterobimetallic chain compounds of general formula $[MnCu(L^x)_2]\cdot m$DMSO (**1a–3a**) and $[CoCu(L^x)_2]\cdot m$DMSO (**1b–3b**) were obtained by reaction of the corresponding sodium salt of the mononuclear Cu^{II} precursor and Mn^{II} or Co^{II} nitrate, respectively, in hot DMSO (Scheme 2c). Alternatively, single crystals of cobalt(II)–copper(II) chain compounds $[CoCu(L^2)_2(H_2O)_2]$ (**2b′**) and $[CoCu(L^3)_2(H_2O)_2]\cdot 4H_2O$ (**3b′**) were grown by slow diffusion in an H-shaped tube of aqueous solutions containing stoichiometric amounts of Co^{II} nitrate in one arm and the corresponding sodium salt of the mononuclear Cu^{II} precursor in the other (Scheme 2c′). All our attempts to get X-ray-

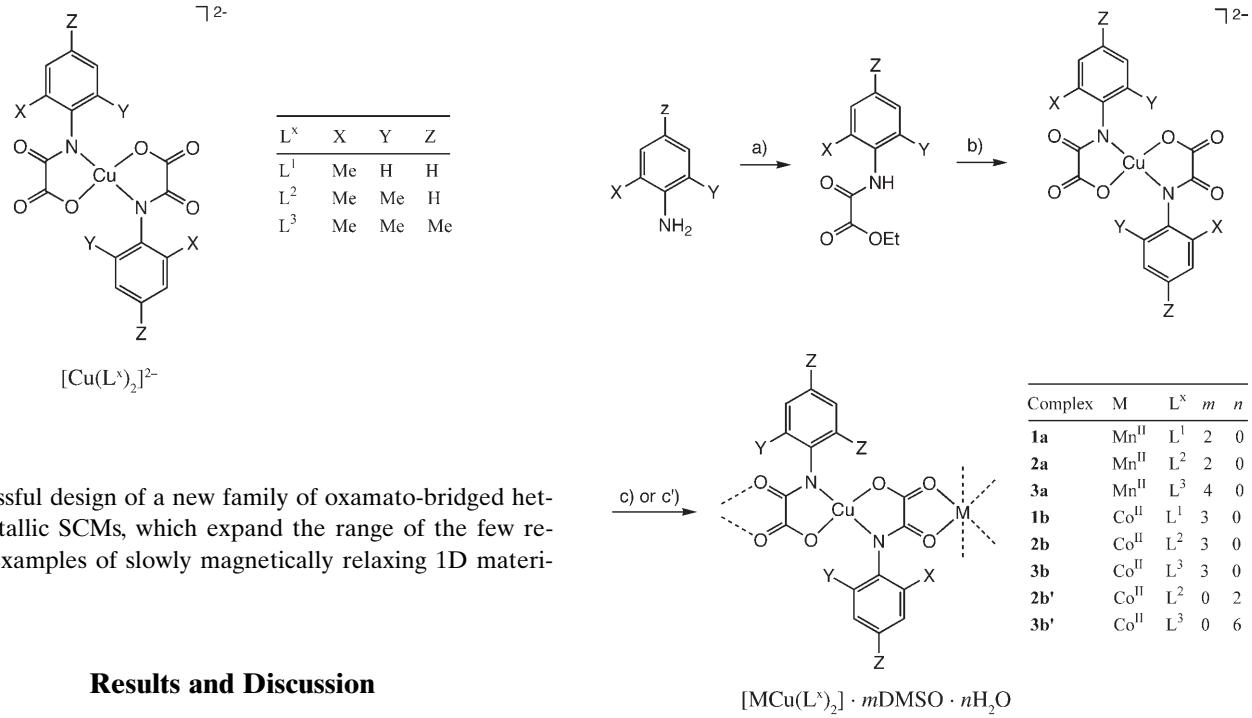

L^x	X	Y	Z
L^1	Me	H	H
L^2	Me	Me	H
L^3	Me	Me	Me

Complex	M	L^x	*m*	*n*
1a	Mn^{II}	L^1	2	0
2a	Mn^{II}	L^2	2	0
3a	Mn^{II}	L^3	4	0
1b	Co^{II}	L^1	3	0
2b	Co^{II}	L^2	3	0
3b	Co^{II}	L^3	3	0
2b'	Co^{II}	L^2	0	2
3b'	Co^{II}	L^3	0	6

Scheme 2. Synthetic pathway to the oxamato-bridged heterobimetallic chain compounds. a) C_2O_2ClOEt, THF (70°C); b) $NaOH/Cu^{II}(NO_3)_2$, H_2O (RT); c) $M^{II}(NO_3)_2$ (M = Co, Mn), DMSO (60°C) or c′) $Co^{II}(NO_3)_2$, H_2O (RT).

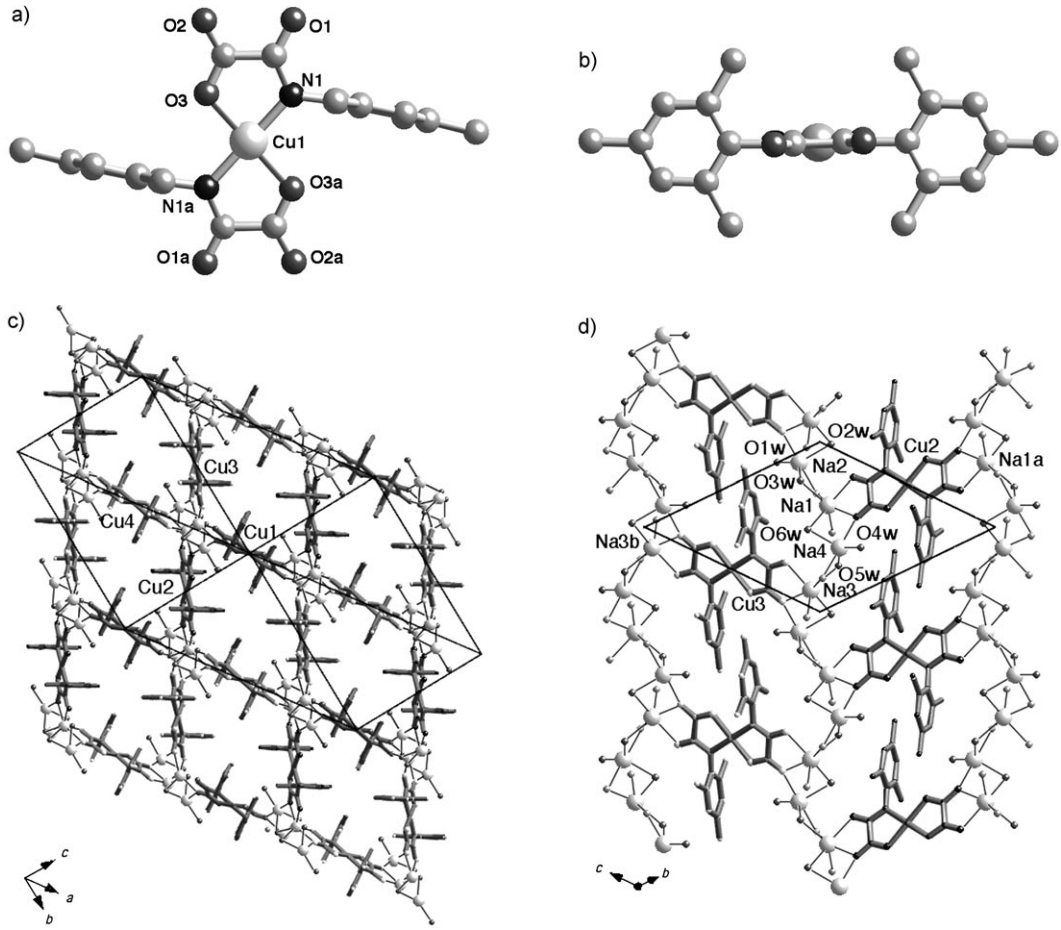

Figure 1. a) Top and b) side views of the mononuclear complex anion of $Na_2[Cu(L^3)_2]\cdot 6H_2O$ with atom labelling for the metal coordination environment. Hydrogen atoms are omitted for clarity. c) and d) Crystal packing of $Na_2[Cu(L^3)_2]\cdot 6H_2O$ along the $[1\bar{1}1]$ and [100] directions. Coordinative bonds to sodium are represented by solid lines (symmetry codes: a = $-x$, $1-y$, $1/2-z$; b = $1/2-x$, $-y$, $1/2-z$).

quality single crystals of the cobalt(II)–copper(II)–L^1 chain analogue were unsuccessful.

The chemical identity of the ligands, the mononuclear copper(II) complexes and the chain compounds was confirmed by elemental analysis (C, H, N, S) and IR and ^{1}H NMR spectroscopy. Analytical and general spectroscopic data are listed in the Supporting Information in Tables S1–S3.

Description of the structures

$Na_2[Cu(L^3)]\cdot 6H_2O$: $Na_2[Cu(L^3)]\cdot 6H_2O$ consists of centrosymmetric mononuclear dianionic copper(II) units $[Cu(L^3)_2]^{2-}$ (Figure 1a), coordinated sodium cations, and both coordinated and crystallisation water molecules. Selected bond lengths and angles are summarised in Table 1.

There are four crystallographically independent copper atoms Cu1–Cu4, which are geometrically equivalent with almost identical bond lengths and angles for the metal coordination environment. The copper atoms are four-coordinate with two amidate-nitrogen and two carboxylate-oxygen atoms from the two oxamate ligands in a *trans* arrangement

Table 1. Selected bond lengths [Å] and angles [°] of $Na_2[Cu(L^3)_2]\cdot 6H_2O$.[a,b]

Cu1–N1a	1.922(4)	Cu3–N3	1.920(4)
Cu1–N1	1.922(4)	Cu3–N3c	1.920(4)
Cu1–O3a	1.955(3)	Cu3–O9c	1.955(3)
Cu1–O3	1.955(3)	Cu3–O9	1.955(3)
Cu2–N2	1.923(4)	Cu4–N4	1.917(4)
Cu2–N2b	1.923(4)	Cu4–N4d	1.917(4)
Cu2–O6b	1.953(3)	Cu4–O12d	1.954(3)
Cu2–O6	1.953(3)	Cu4–O12	1.954(3)
N1a-Cu1-N1	180.0	N3-Cu3-N3c	180.0
N1a-Cu1-O3	95.77(15)	N3-Cu3-O9	84.14(15)
N1-Cu1-O3	84.23(15)	N3c-Cu3-O9	95.86(15)
N1a-Cu1-O3a	84.22(15)	N3-Cu3-O9c	95.86(15)
N1-Cu1-O3a	95.78(15)	N3c-Cu3-O9	84.14(15)
O3-Cu1-O3a	180.0	O9-Cu3-O9c	180.0
N2-Cu2-N2b	180.0	N4-Cu4-N4d	180.0
N2-Cu2-O6b	95.80(15)	N4-Cu4-O12c	95.52(15)
N2c-Cu2-O6	84.20(15)	N4d-Cu4-O4d	84.48(15)
N2-Cu2-O6	84.20(15)	N4-Cu4-O12	84.48(15)
N2b-Cu2-O6	95.80(15)	N4d-Cu4-O12	95.52(15)
O6b-Cu2-O6	180.0	O12d-Cu4-O12	180.0

[a] Estimated standard deviations are given in parentheses. [b] Symmetry codes: a = $-x$, $-y$, $-z$; b = $-x$, $-y$, $-z-1$; c = $-x-1$, $-y$, $-z+1$; d = $-x$, $-y-1$, $-z-1$.

building a square-planar surrounding. The average Cu–N and Cu–O bond lengths are 1.921(2) and 1.954(3) Å, respectively, and they compare well with those reported earlier for related square-planar copper(II) complexes with two oxamate ligands in *cis* arrangement (average Cu–N and Cu–O bond lengths of 1.910 and 1.945 Å, respectively).[16] The average dihedral angle between the basal plane of the copper atoms and the planes of the oxamato groups is 1.4(2)°. The phenyl rings are practically perpendicular to the oxamate groups to prevent steric repulsion between the 2- and 6-methyl substituents and the carbonyl oxygen atoms (Figure 1b). The average dihedral angle between their mean planes is 82.1(4)°. More likely, the alternative *cis* arrangement of the oxamate ligands is precluded because of steric hindrance between the trimethyl-substituted phenyl groups. In this regard, it is important to point out that the *trans* arrangement of the oxamate ligands in $Na_2[Cu(L^3)_2]\cdot 6H_2O$ is kept in the bimetallic chains as well (see below).

In the crystal lattice, the bis(oxamato)copper(II) entities are coordinated to the sodium atoms through the carbonyl oxygen atoms to form a corrugated 3D rhombic network structure (Figure 1c). The four copper atoms Cu1–Cu4 occupy the centre of each edge of the rhombus, while the four sodium atoms Na1–Na4 define the vertexes. Additional water molecules, both bridging and terminal, complete the coordination sphere of the sodium atoms and thus lead to pillared 1D arrays (Figure 1d). There are both five- and six-coordinate sodium atoms with Na–O distances in the range 2.315(4)–2.439(4) Å. The shortest Cu1···Cu2 distance through the coordinated sodium ions is 7.2667(8) Å.

$[CoCu(L^2)_2(H_2O)_2]$ (2b′): Complex **2b′** consists of neutral oxamato-bridged cobalt(II)–copper(II) zigzag chains (Figure 2a). Within each chain, the bis(oxamato)copper(II) entity acts as a bis-bidentate ligand through the *cis* carbonyl oxygen atoms towards *cis*-diaquacobalt(II) units. Because of the *cis* conformation of the octahedral Co atoms, two different isomers (Δ and Λ) exist that alternate regularly along the chain and thus lead to an achiral zigzag chain structure. A chiral helical chain structure would result in the case of identical isomers (Δ or Λ). Selected bond lengths and angles for **2b′** are summarised in Table 2.

The copper atom is four-coordinate with two amidate-nitrogen and two carboxylate-oxygen atoms from the two oxamate ligands in a *trans* arrangement building a square-planar surrounding (Cu1–N1 1.926(3), Cu1–O3 1.956(3) Å). The dihedral angle between the basal plane of the copper atom and the plane of the oxamato groups is 2.85(12)°. The cobalt atom is six-coordinate with two *cis*-coordinated water molecules and four carbonyl oxygen atoms from two oxamate ligands forming a distorted octahedral surrounding. The bond lengths around the cobalt atom (Co1–O1w 2.073(5), Co1–O1 2.118(3), Co1–O2 2.082(3) Å) are similar to those observed for the high-spin Co^{II} ion in the related oxamato-bridged cobalt(II)–copper(II) chain [CoCu(opba)-(dmso)$_3$] (opba = *o*-phenylenebis(oxamate)).[14a] The intrachain Co1···Cu1 separation through the oxamato bridge in **2b′** is 5.296(1) Å, a value which compares well with that reported for [CoCu(opba)(dmso)$_3$] (5.336(1) Å).[14a]

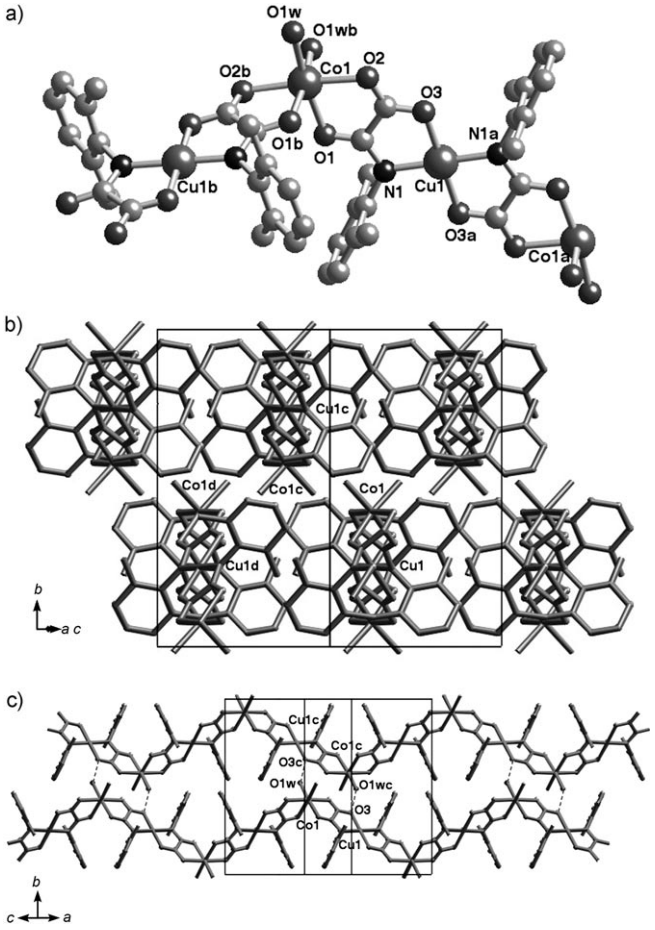

Figure 2. a) View of a fragment of the chain of **2b′** with atom labelling for the metal coordination environments. Hydrogen atoms are omitted for clarity. b) and c) Crystal packing of the chains of **2b′** along the [10$\bar{1}$] and [101] directions. Hydrogen bonds are represented by dashed lines (symmetry codes: a = 1/2−*x*, 1/2−*y*, −*z*; b = −*x*, *y*, 1/2−*z*; c = *x*, 1−*y*, 1−*z*; d = *x*, *y*, 1/2−*z*).

Table 2. Selected bond lengths [Å] and angles [°] of **2b′**.[a,b]

Cu1–N1	1.923(4)	Cu1–N1a	1.923(4)
Cu1–O3	1.958(3)	Cu1–O3a	1.958(3)
Co1–O1	2.083(3)	Co1–O1b	2.083(3)
Co1–O2	2.123(3)	Co1–O2b	2.123(3)
Co1–O1w	2.076(4)	Co1–O1wb	2.076(4)
O1w-Co1-O1wb	92.1(3)	O1w-Co1-O1	170.09(14)
O1wb-Co1-O1	92.4(2)	O1w-Co1-O1b	92.4(2)
O1-Co1-O1w	170.09(14)	O1-Co1-O1b	84.5(2)
O1w-Co1-O2	91.15(14)	O1wb-Co1-O2	91.03(14)
O1-Co1-O2	79.95(12)	O1b-Co1-O2	97.69(12)
O1wb-Co1-O2	91.03(14)	O1wb-Co1-O2b	91.15(14)
O1-Co1-O2b	97.69(12)	O1b-Co1-O2b	79.95(12)
O2-Co1-O2b	176.8(2)	N1-Cu1-N1a	180.0
N1-Cu1-O3a	95.09(14)	N1a-Cu1-O3a	84.91(14)
N1-Cu1-O3	84.91(14)	N1a-Cu1-O3	95.09(14)
O3a-Cu1-O3	180.0		

[a] Estimated standard deviations are given in parentheses. [b] Symmetry codes: a = −*x*+1/2, −*y*+1/2, −*z*; b = −*x*, *y*, −*z*+1/2.

The chains of **2b′** grow parallel to the [10$\bar{1}$] direction and they are rather well separated from each other (Figure 2b). The phenyl rings are practically perpendicular to the oxamate groups (the dihedral angle between their mean planes is 85.6(2)°) and thus afford effective shielding between the copper atoms of neighbouring chains in the *ac* plane. However, the *cis* conformation of the octahedral cobalt units prevents the aromatic rings from arranging alternately in the two perpendicular directions to the basal plane of the copper atoms, and this facilitates approach between the cobalt atoms of neighbouring chains (Figure 2c). This leads to weak interchain hydrogen-bonding interactions involving the coordinated water molecules and the carbonyl oxygen atoms of the oxamate ligands (O1w···O3c 2.867(4) Å, Figure 2c). The shortest interchain Co1···Co1c and Cu1···Co1c distances are 5.995(5) and 6.628(3) Å, respectively (symmetry code: c = $-x$, $-y$, $1-z$).

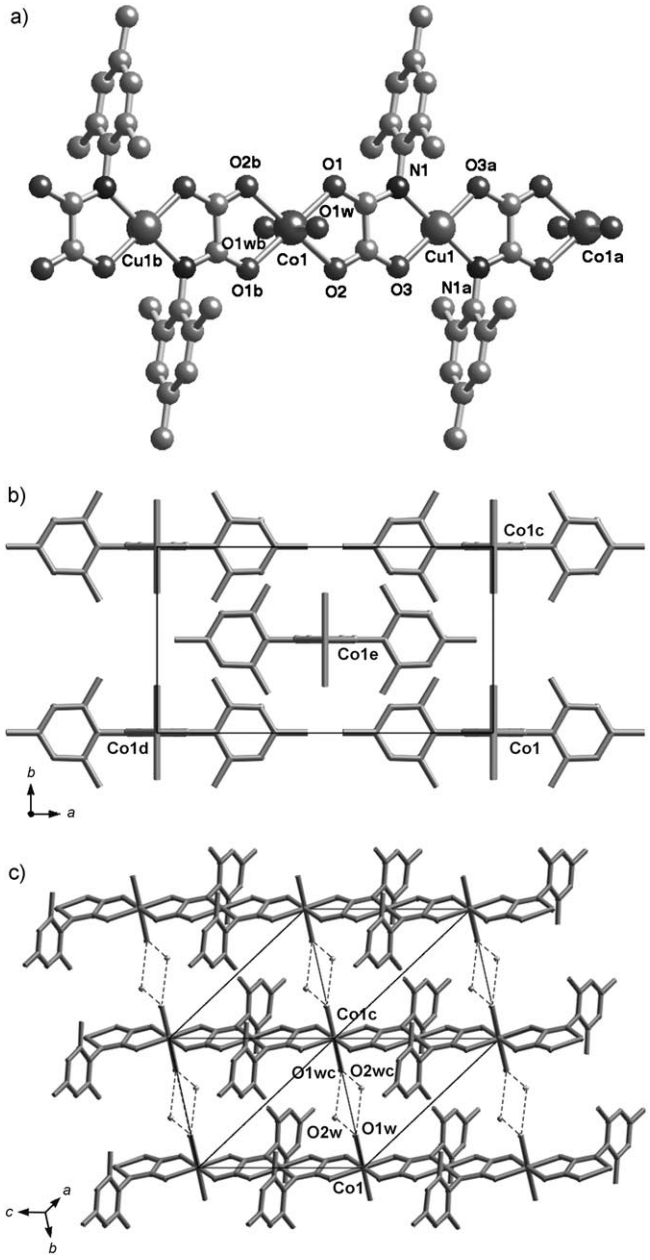

Figure 3. a) View of a fragment of the chain of **3b′** with atom labelling for the metal coordination environments. Hydrogen atoms are omitted for clarity. b) and c) Crystal packing of the chains of **3b′** along the [001] and [111] directions. Hydrogen bonds are represented by dashed lines (symmetry codes: a = $-x$, y, $-z$; b = $-x$, y, $1-z$; c = x, $1+y$, z; d = $1+x$, y, z; e = $1/2-x$, $1/2-y$, $-z$).

$[CoCu(L^3)_2(H_2O)_2]\cdot 4H_2O$ (3b′): Complex **3b′** consists of neutral oxamato-bridged cobalt(II)–copper(II) linear chains (Figure 3a) and water molecules of crystallisation. Within each chain, the bis(oxamato)copper(II) entity acts as a bis-bidentate ligand through the *cis* carbonyl oxygen atoms towards *trans*-diaquacobalt(II) units. This situation contrasts with that of **2b′**, where *cis* coordination of the two water molecules to cobalt atoms leads to a zigzag chain structure. A precedent exists in the literature of two related oxamato-bridged manganese(II)–copper(II) chains $[MnCu(opba)(H_2O)_2]\cdot DMSO$ and $[MnCu(opba)(dmso)_3]$, which adopt linear and zigzag structures, respectively.[14b,c] Selected bond lengths and angles for **3b′** are summarised in Table 3.

Table 3. Selected bond lengths [Å] and angles [°] of **3b′**.[a,b]

Cu1−N1	1.949(3)	Cu1−N1a	1.949(3)
Cu1−O3	1.958(3)	Cu1−O3a	1.958(3)
Co1−O1	2.066(3)	Co1−O1b	2.066(3)
Co1−O2	2.109(3)	Co1−O2b	2.109(3)
Co1−O1w	2.158(5)	Co1−O1wb	2.158(5)
N1-Cu1-N1a	180.0	N1-Cu1-O3a	95.45(12)
N1a-Cu1-O3a	84.55(12)	N1-Cu1-O3	84.55(12)
N1a-Cu1-O3	95.45(12)	O3a-Cu1-O3	180.0
O1-Co1-O1b	180.0	O1-Co1-O2b	98.93(12)
O1b-Co1-O2b	81.07(12)	O1-Co1-O2	81.07(12)
O1b-Co1-O2	98.93(12)	O2b-Co1-O2	180.0
O1-Co1-O1wb	90.0	O1b-Co1-O1wb	90.0
O2b-Co1-O1wb	90.0	O2-Co1-O1wb	90.0
O1-Co1-O1w	90.0	O1b-Co1-O1w	90.0
O2b-Co1-O1w	90.0	O2-Co1-O1w	90.0
O1wb-Co1-O1w	180.0		

[a] Estimated standard deviations are given in parentheses. [b] Symmetry codes: a = $-x$, y, $-z$; b = $-x$, y, $1-z$.

The copper atom is four-coordinate with two amidate-nitrogen and two carboxylate-oxygen atoms from the two oxamate ligands in a *trans* arrangement building a square-planar environment. The bond lengths around the copper atom (Cu1−N1 1.949(3), Cu1−O3 1.958(3) Å) are close to those of the monomeric precursor $Na_2[Cu(L^3)_2]\cdot 6H_2O$. The cobalt atom is six-coordinate with two *trans*-coordinated water molecules and four carbonyl oxygen atoms from two oxamate ligands forming a distorted octahedral surrounding. The bond lengths around the cobalt atom (Co1−O1w 2.158(5), Co1−O1 2.109(3), Co1−O2 2.066(3) Å) are similar to those observed for **2b′**.

The chains of **3b′** grow parallel to the [001] direction and they are well separated from each other (Figure 3b). The phenyl rings are practically perpendicular to the oxamate

groups (the dihedral angle between their mean planes is 89.7(2)°) and thus afford effective shielding between neighbouring chains in the *ab* plane. There are, however, some weak interchain hydrogen-bonding interactions along the *b* axis in **3b′** involving the coordinated and the crystallisation water molecules (O1w···O2w 2.878(6) Å), which form a hydrogen-bonded square motif (Figure 3c). The intrachain Co1···Cu1 distance across bridging oxamato ligand in **3b′** is 5.3010(15) Å, a value which is much shorter than the shortest interchain metal–metal separation of 8.702(3) Å for Co1···Co1c and Cu1···Cu1c (symmetry code: c = x, $1+y$, z).

Magnetic properties

Manganese(II)–copper(II) chains: The dc magnetic properties of **1a**–**3a** in the form of $\chi_M T$ versus T plots (χ_M is the magnetic susceptibility per MnCu pair) are shown in Figure 4a. The values of $\chi_M T$ at room temperature vary in the narrow range 4.31–4.35 $cm^3 mol^{-1} K$, and they are lower than expected for the sum of a square-planar Cu^{II} ion ($S_{Cu}=1/2$, $\chi_M T = 0.40\ cm^3 mol^{-1} K$ with $g=2.1$) and an octahedral high-spin Mn^{II} ion ($S_{Mn}=5/2$, $\chi_M T = 4.38\ cm^3 mol^{-1} K$ with $g=2.0$) in magnetic isolation. This suggests relatively large intrachain antiferromagnetic interaction between the Cu^{II} and Mn^{II} ions through the oxamate bridge. On cooling, $\chi_M T$ decreases and attains a minimum around 125 K for **1a** and **2a** and at 105 K for **3a** (inset of Figure 4a). The presence of a minimum is characteristic of ferrimagnetic manganese(II)–copper(II) chain compounds.[3a,14b,c] The $\chi_M T$ value reaches a maximum at about 2.0 K for **1a** and **2a** and at 6.8 K for **3a**, with $\chi_M T$ values in the range 10.5–24.0 $cm^3 mol^{-1} K$, due to saturation effects. The lack of a maximum in χ_M allows us to rule out the occurrence of 3D long-range antiferromagnetic order and thus suggests that the chains are magnetically well isolated.

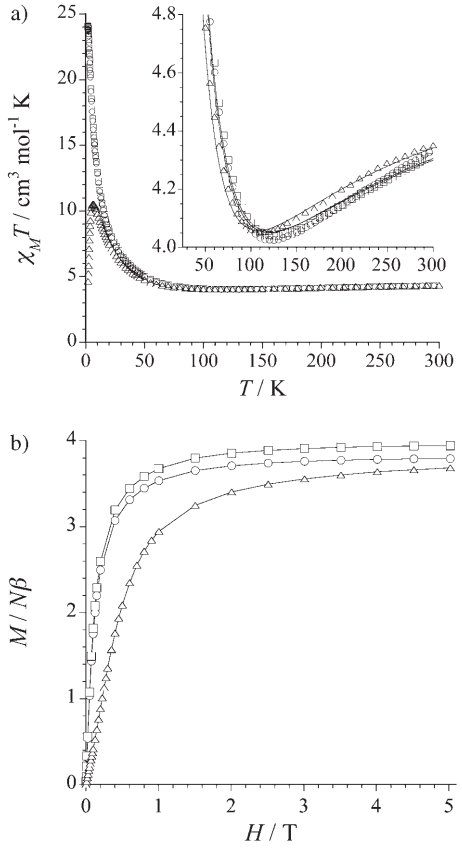

Figure 4. a) Temperature dependence of $\chi_M T$ of **1a** (○), **2a** (□) and **3a** (△) in an applied magnetic field of 1 T ($T \geq 50$ K) and 250 G ($T < 50$ K). The inset shows the minimum of $\chi_M T$. The solid lines are the best-fit curves (see text). b) Field dependence of M of **1a** (○), **2a** (□) and **3a** (△) at 2.0 K. The solid lines are guides for the eye.

The M versus H plots for **1a**–**3a** at 2.0 K (M is the magnetisation per MnCu pair and H the applied magnetic field) are shown in Figure 4b. The magnetisation values at 5 T are in the range 3.70–3.95 $N\beta$ and they are consistent with the predicted value ($M_s = 3.90 N\beta$) for an $S=2$ state resulting from antiferromagnetic coupling between a high-spin Mn^{II} ion ($S_{Mn}=5/2$ with $g=2.0$) and a Cu^{II} ion ($S_{Cu}=1/2$ with $g=2.1$). Moreover, the magnetisation isotherms show fast saturation with about 90% of M_s being reached in a field of 1000 G. This reveals strong short-range correlation along the chain favouring antiparallel alignment of the spins of Cu^{II} and Mn^{II} ions.

The magnetic susceptibility data of **1a**–**3a** were analysed by using the one-dimensional model developed by Kahn et al.[3a] In this model, the Mn^{II} and Cu^{II} ions are treated as classic ($S_{Mn}=5/2$) and quantum ($S_{Cu}=1/2$) spins, respectively. The spin Hamiltonian is $\mathbf{H} = \sum_i [-J\mathbf{S}_{Mn,i}\mathbf{S}_{Cu,i} + \beta H(g_{Mn}\mathbf{S}_{Mn,i} + g_{Cu}\mathbf{S}_{Cu,i})]$, where i runs over the MnCu units, J is the exchange coupling between neighbouring spins and g_{Mn} and g_{Cu} are the Landé factors. Least-squares fitting of the experimental data through this model in the temperature range 30–300 K gave $-J$ values of 27.9 (**1a**), 28.2 (**2a**) and 24.7 cm^{-1} (**3a**; Table 4). The theoretical curves reproduce very well the observed minima in the $\chi_M T$ versus T plots (solid lines in the inset of Figure 4a). The antiferromagnetic coupling between Cu^{II} and Mn^{II} ions through the oxamate bridge in **1a** and **2a** is somewhat stronger than in **3a**. This suggests that the copper atoms in **1a** and **2a** are square-planar, whereas that in **3a** is square-pyramidal with an apical DMSO ligand, as previously reported for the related chain $[MnCu(opba)(dmso)_3]$.[14c] In the former case, the copper atom lies in the oxamato plane (CuN_2O_2 chromophore), whereas it is out of this mean plane in the latter case (CuN_2O_3 chromophore). This leads to better overlap of

Table 4. Selected dc magnetic data for the $Mn^{II}Cu^{II}$ chain compounds.

Complex	$-J$ [cm^{-1}][a]	g_{Mn}	g_{Cu}
1a	27.9	2.00	2.09
2a	28.2	2.00	2.07
3a	24.7	2.00	2.06

[a] J is the exchange coupling parameter.

the magnetic orbitals of Cu^{II} and Mn^{II} ions through the σ in-plane exchange pathway of the oxamate bridge, and thus to a larger antiferromagnetic coupling.

The *ac* magnetic measurements for **1a–3a** showed no evidence of slow magnetic-relaxation effects. In fact, no out-of-phase magnetic susceptibility signals were observed above 2.0 K for these compounds (data not shown). This is likely due to the magnetically isotropic character of the octahedral high-spin Mn^{II} ion ($^6A_{1g}$, D value close to zero).

Cobalt(II)–copper(II) chains: The dc magnetic properties of **1b–3b** in the form of $\chi_M T$ versus T plots (χ_M is the magnetic susceptibility per CoCu pair) are shown in Figure 5a, and

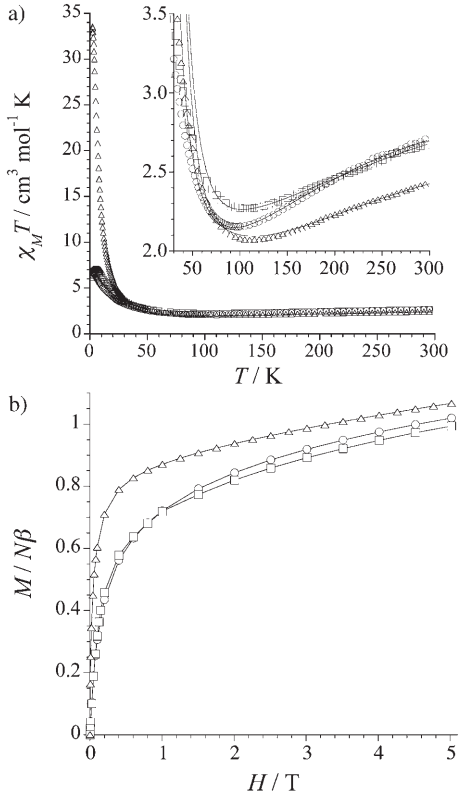

Figure 5. a) Temperature dependence of $\chi_M T$ of **1b** (○), **2b** (□) and **3b** (△) in an applied magnetic field of 1 T ($T \geq 50$ K) and 250 G ($T < 50$ K). The inset shows the minimum of $\chi_M T$. The solid lines are the best-fit curves (see text). b) Field dependence of M of **1b** (○), **2b** (□) and **3b** (△) at 2.0 K. The solid lines are guides to the eye.

those of **2b′** and **3b′** in Figure 6a. The $\chi_M T$ values at room temperature vary in the range 2.42–2.70 cm^3 mol^{-1} K and they are smaller than expected for the sum of a square-planar Cu^{II} ion ($S_{Cu} = 1/2$, $\chi_M T = 0.40$ cm^3 mol^{-1} K with $g = 2.1$) and an octahedral high-spin Co^{II} ion ($S_{Co} = 3/2$) with an orbitally degenerate $^4T_{1g}$ single-ion ground state ($\chi_M T = 2.5$–3.0 cm^3 mol^{-1} K)[17] in magnetic isolation. This suggests the occurrence of a relatively large intrachain antiferromagnetic interaction between the Cu^{II} and the Co^{II} ions through the oxamate bridge. On cooling, $\chi_M T$ decreases and it attains a

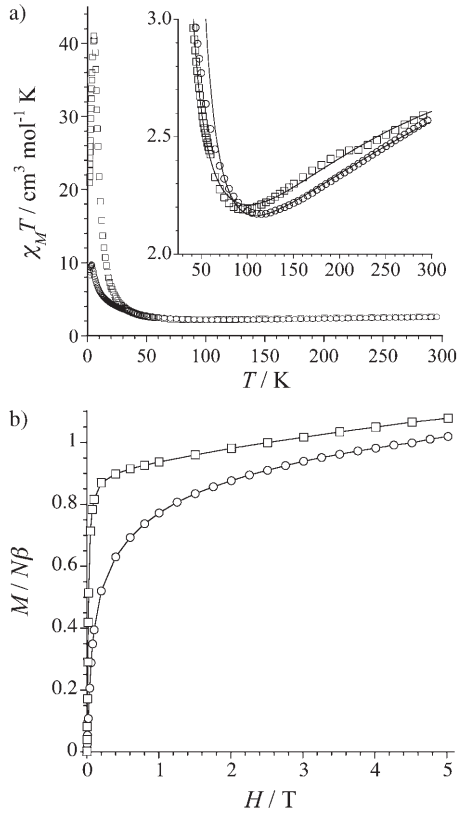

Figure 6. a) Temperature dependence of $\chi_M T$ of **2b′** (○) and **3b′** (□) in an applied magnetic field of 1 T ($T \geq 50$ K) and 250 G ($T < 50$ K). The inset shows the minimum of $\chi_M T$. The solid lines are the best-fit curves (see text). b) Field dependence of M of **2b′** (○) and **3b′** (□) at 2.0 K. The solid lines are guides for the eye.

minimum in the temperature range 90–115 K (insets of Figures 5a and 6a), which is typical of ferrimagnetic cobalt(II)–copper(II) chain compounds.[3b,14a] The $\chi_M T$ value reaches a maximum at about 2–9 K, with $\chi_M T$ values in the range 7.5–40.0 cm^3 mol^{-1} K, which is due to magnetic anisotropy and saturation effects. As for their manganese(II)–copper(II) analogues **1a–3a**, the lack of a maximum in χ_M allows us to rule out 3D long-range antiferromagnetic order and thus suggests that the chains are magnetically well isolated from each other.

The M versus H plots for **1b–3b** at 2.0 K (M is the magnetisation per CoCu pair) are shown in Figure 5b, and those of **2b′** and **3b′** in Figure 6b. The magnetisation values at 5 T vary in the range 0.98–1.10 $N\beta$ and they are consistent with the predicted value ($M_s = 1.10\,N\beta$) for partial spin cancellation resulting from antiferromagnetic coupling between a high-spin Co^{II} ion ($S_{eff} = 1/2$ with $g = 4.2$) and a Cu^{II} ion ($S = 1/2$ with $g = 2.1$). Moreover, the magnetisation isotherms show fast saturation with about 80% of the value of M_S being reached in a field of 1000 G. This reveals a strong short-range correlation along the chain favouring antiparallel alignment of the spins of Cu^{II} and Co^{II} ions.

To analyse the magnetic susceptibility data of **1b–3b**, **2b′** and **3b′**, in which the octahedral high-spin Co^{II} ions are orbi-

tally degenerate ($^4T_{1g}$), we used the branch chain model previously developed by Kahn et al. for the related oxamato-bridged chain $[CoCu(pbaOH)(H_2O)_3]\cdot 2H_2O$.[3b] This model assumes that only z components of spin and orbital momenta are coupled and that the applied magnetic field is along the quantisation axis. The corresponding Hamiltonian is $\mathbf{H}=\sum_i [-J\mathbf{S}_{Co,i(z)}\mathbf{S}_{Cu,i(z)}+J'\mathbf{L}_{Co,i(z)}\mathbf{S}_{Co,i(z)}+D\mathbf{L}^2_{Co,i(z)}-\beta H_{(z)}\cdot(g_{Co}\mathbf{S}_{Co,i(z)}+g_{Cu}\mathbf{S}_{Cu,i(z)}+k\mathbf{L}_{Co,i(z)})]$, where i runs over the CoCu units, J and J' are the exchange and spin-orbit coupling parameters, k and D the orbital reduction and local anisotropy parameters of the cobalt(II) ion, and g_{Co} and g_{Cu} the Landé factors. Least-squares fitting of the experimental data through this model in the temperature range 30–300 K gave $-J$ values in the range 35.0–45.8 cm^{-1} for **1b**–**3b**, **2b′** and **3b′** (Table 5). The theoretical curves reproduce quite well the observed minima in the $\chi_M T$ versus T plots (solid lines in the inset of Figures 5a and 6a). The antiferromagnetic coupling between Cu^{II} and Co^{II} ions through the oxamato bridges in **1b**–**3b**, **2b′** and **3b′** is somewhat stronger than that reported for $[CoCu(pbaOH)(H_2O)_3]\cdot 2H_2O$ ($-J=18.0\ cm^{-1}$).[3b] As mentioned above, this is likely due to the fact that the copper atom in these chains lies in the oxamato plane (CuN_2O_2 chromophore in a square-planar surrounding), as evidenced from the X-ray crystal structures of **2b′** and **3b′**, whereas it lies out of this mean plane in $[CoCu(pbaOH)(H_2O)_3]\cdot 2H_2O$ (CuN_2O_3 chromophore in a square-pyramidal environment). The effective spin–orbit coupling can be related with the spin–orbit coupling parameter λ through the expression $J'=-Ak\lambda$. This gives values of $-\lambda$ in the range 82–110 cm^{-1} (with $A=3/2$) for **1b**-**3b**, **2b′** and **3b′** (Table 5; cf. $\lambda=-180\ cm^{-1}$ for the free ion). The local magnetic anisotropy parameter D is related to the energy splitting of the orbital triplet ground state $^4T_{1g}$ resulting from axial distortion of the octahedral geometry of the Co^{II} ion. The large values of D in the range 538–719 cm^{-1} for **1b**-**3b**, **2b′** and **3b′** (Table 5) are similar to those reported for other axially distorted six-coordinate high-spin cobalt(II) complexes.[17]

Table 5. Selected dc magnetic data for the $Co^{II}Cu^{II}$ chain compounds.

Complex	$-J$ [cm^{-1}][a]	g_{Co}	g_{Cu}	$-\lambda$ [cm^{-1}][b]	k[c]	D [cm^{-1}][d]
1b	40.3	2.24	2.08	110	0.98	538
2b	40.5	2.30	2.07	107	0.97	719
3b	44.3	2.21	2.08	99	0.95	710
2b′	45.8	2.24	2.09	82	0.94	692
3b′	35.0	2.38	2.05	110	0.80	610

[a] J is the exchange coupling parameter. [b] λ is the spin–orbit coupling parameter ($A=3/2$). [c] k is the orbital reduction parameter. [d] D is the local anisotropy parameter.

The ac magnetic properties of this series of cobalt(II)–copper(II) chain compounds show evidence of slow magnetic-relaxation effects which are typical of SCMs in all cases except for **1b**. The χ_M' and χ_M'' versus T plots for **2b**, **2b′**, **3b** and **3b′** (χ_M' and χ_M'' are the in-phase and out-of-phase magnetic susceptibilities per CoCu pair, respectively) are shown in Figures 7–10. The χ_M'' value becomes nonzero below 3.5 K for **2b**, and shows a maximum at 2.1 K for the highest

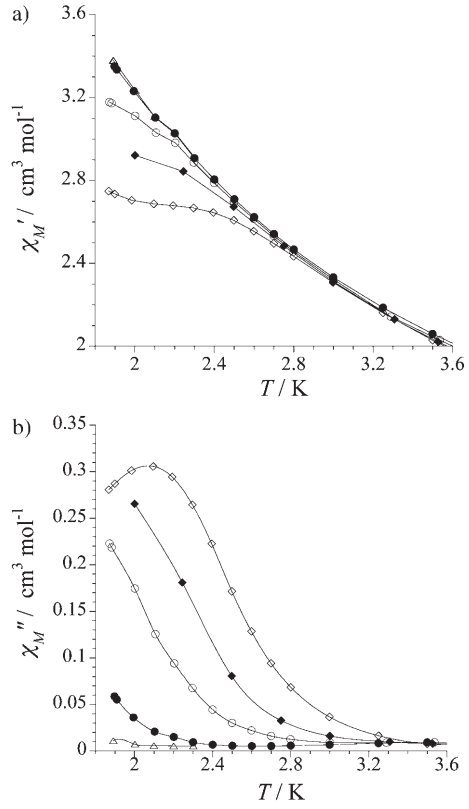

Figure 7. Temperature dependence of a) χ_M' and b) χ_M'' of **2b** in zero applied static field and under 1 G oscillating field at different frequencies of the oscillating field: 1 (△), 10 (●), 100 (○), 333 (◆), 1000 Hz (◇). The solid lines are guides for the eye.

applied frequency ($\nu=1000$ Hz; Figure 7b). For the analogue **2b′**, χ_M'' becomes nonzero below 3.0 K, but no χ_M'' maxima are observed above 2.0 K (Figure 8b), which is the lowest temperature in our susceptometer. On the contrary, χ_M'' shows maxima between 3.5 ($\nu=1400$ Hz) and 2.2 K ($\nu=300$ Hz) for **3b** (Figure 9b). For the analogue **3b′**, the χ_M'' maxima are located at lower temperatures between 2.3 ($\nu=1400$ Hz) and 2.0 K ($\nu=300$ Hz; Figure 10b). Overall, the temperature T_{max} of the maxima of χ_M'' along this series of cobalt(II)–copper(II)–L^x chain compounds varies according to the steric hindrance of the aromatically substituted oxamate ligand in the series $L^1<L^2<L^3$. It appears that the interchain interactions, which are always present whatever the compound, as revealed by the crystal structures of **2b′** and **3b′**, may tune the dynamic magnetic properties by lowering the blocking temperature with respect to that expected for a perfectly isolated chain. Although this hypothesis has no precedent in the relatively recent literature on SCMs,[5,9–13] there are some studies that point out the influence of intermolecular interactions on the dynamic behaviour of related SMMs.[18–20]

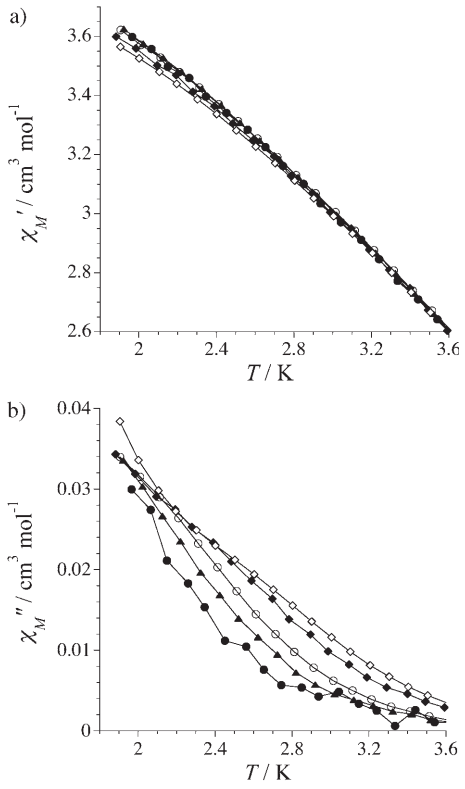

Figure 8. Temperature dependence of a) χ_M' and b) χ_M'' of **2b′** in zero applied static field and under 1 G oscillating field at different frequencies of the oscillating field: 10 (●), 30 (▲), 100 (○), 333 (◆), 1000 Hz (◇). The solid lines are guides for the eye.

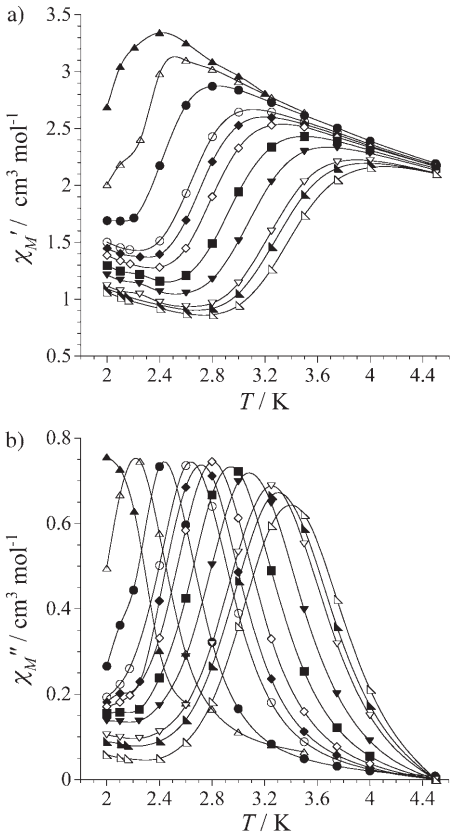

Figure 9. Temperature dependence of a) χ_M' and b) χ_M'' of **3b** in zero applied static field and under 1 G oscillating field at different frequencies of the oscillating field: 0.1 (▲), 1 (△), 10 (●), 50 (○), 75 (◆), 100 (◇), 200 (■), 400 (▼), 700 (▽), 1000 (▶), 1400 Hz (▷). The solid lines are guides for the eye.

The relaxation time τ for **3b** and **3b′** can be calculated from the maximum of χ_M'' at a given frequency ν, whereby it is assumed that switching of the oscillating ac field matches the relaxation rate of the magnetisation ($1/\tau = 2\pi\nu$). The calculated τ values at T_{max} follow the Arrhenius law characteristic of a thermally activated mechanism: $\tau = \tau_0 \exp(E_a/k_B T)$ (Figure 11 a). The activation energies E_a are 38.0 (**3b**) and 16.3 cm^{-1} (**3b′**), and the preexponential factors τ_0 2.3×10^{-11} (**3b**) and 4.0×10^{-9} s (**3b′**; Table 6). As expected, the larger the antiferromagnetic intrachain coupling [$-J = 44.3$ (**3b**) and 35.0 cm^{-1} (**3b′**)], the greater the activation energy to reverse the magnetisation direction. However, these values must be regarded with caution because of the very narrow temperature range available for both cobalt(II)–copper(II)–L^3 chain compounds. Indeed, the χ_M'' versus χ_M' plot at 2.0 K for **3b** and **3b′** (Cole–Cole plot[21a]) in the frequency range 1–1400 Hz gives a semicircle in both cases (Figure 11 b). The least-squares fit of the experimental data through the Cole–Cole expression[21], $\chi = \chi_S + (\chi_T - \chi_S)/[1 + (i\omega\tau)^{1-\alpha}]$ gave very small values for the α parameter of 0.10 for **3b** and 0.05 for **3b′** ($\alpha = 0$ for an ideal Debye model with a single relaxation time); thus, spin-glass behaviour is ruled out.[22] The adiabatic (χ_S) and isothermal (χ_T) susceptibilities are 0.5 and 3.1 cm^3 mol^{-1} for **3b** and 0.1 and 4.7 cm^3 mol^{-1} for **3b′**, respectively (Table 6). Moreover, the relative variation of the temperature of the maximum of χ_M'' with respect to the frequency, expressed by the so called F parameter defined by Mydosh as $F = (\Delta T_{max}/T_{max})/\Delta(\lg\nu)$,[22b] is 0.25 for **3b** and 0.12 for **3b′** (Table 6). These moderate values of F are typical of SCMs and they are greater than those expected for spin glasses (F values smaller than 0.01).[22c]

Conclusion

A new family of oxamato-bridged heterobimetallic chains has been obtained through ligand design from the self-assembly of potentially bis-bidentate square-planar copper(II) complexes with sterically hindered aromatically substituted oxamate ligands and transition metal ions such as manganese(II) and cobalt(II). Both manganese(II)–copper(II) and cobalt(II)–copper(II) chains behave as ferrimagnetic chains with moderately strong intrachain antiferromagnetic coupling between Cu^{II} and M^{II} ions (M = Mn and Co) through the oxamate bridge. In spite of this, only the $Co^{II}Cu^{II}$ chains show slow magnetic relaxation effects which are typical of SCMs. Together with the large magnetic anisotropy of the orbitally degenerate octahedral high-spin Co^{II} ion, however,

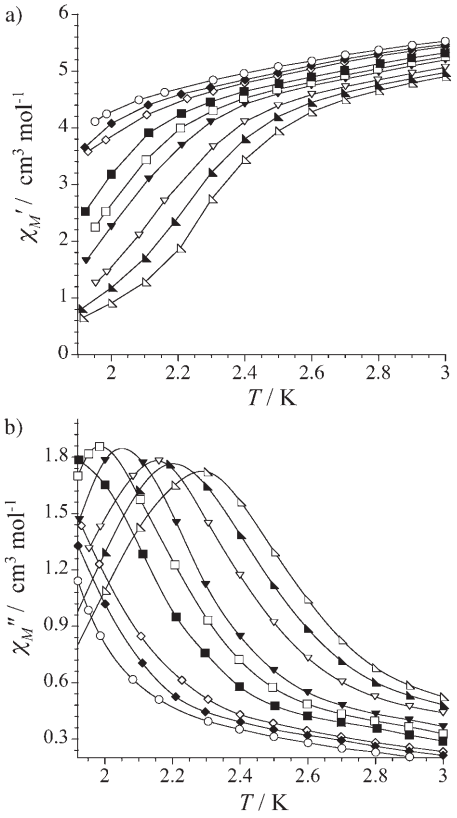

Figure 10. Temperature dependence of a) χ_M' and b) χ_M'' of **3b′** in zero applied static field and under 1 G oscillating field at different frequencies of the oscillating field: 50 (○), 75 (◆), 100 (◇), 200 (■), 300 (□), 400 (▼), 700 (▽), 1000 (▶), 1400 Hz (▷). The solid lines are guides for the eye.

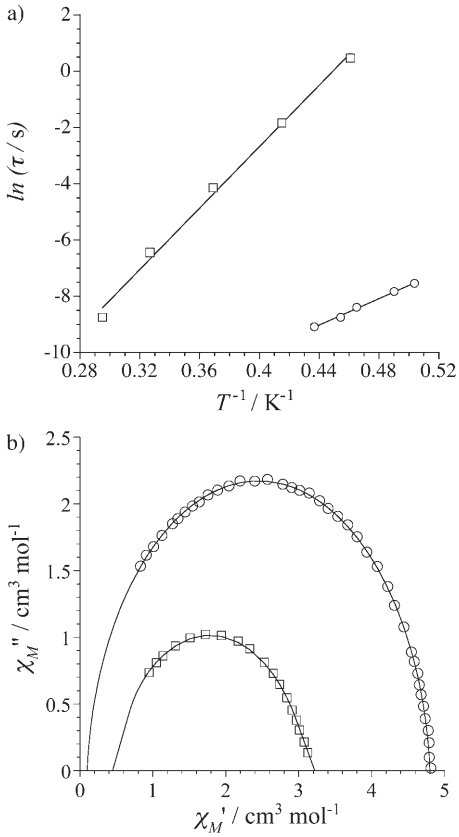

Figure 11. a) Arrhenius plots and b) Cole–Cole plots at 2.0 K for **3b** (□) and **3b′** (○). The solid lines are the best-fit curves (see text).

Table 6. Selected ac magnetic data for $Co^{II}Cu^{II}$ chain compounds **3b** and **3b′**.

Complex	τ_0 [s][a]	E_a [cm^{-1}][b]	α[c]	χ_S [cm^{3}mol^{-1}][d]	χ_T [cm^{3}mol^{-1}][e]	F[f]
3b	2.3×10^{-11}	38.0	0.10	0.5	3.1	0.25
3b′	4.0×10^{-9}	16.3	0.05	0.1	4.7	0.12

[a] τ_0 is the preexponential factor. [b] E_a is the activation energy. [c] α is the Cole–Cole parameter. [d] χ_S is the adiabatic susceptibility. [e] χ_T is the isothermal susceptibility. [f] F is the Mydosh parameter.

certain steric requirements in the Cu^{II} precursor must be fulfilled in order to observe SCM behaviour at sufficiently high temperatures (above 2.0 K). Thus, the overall increase in T_{max} observed in the series of $Co^{II}Cu^{II}$ chains when increasing the number of methyl substituents in the benzene ring from one to three is related to the increased separation between chains and hence decreased interchain interactions. Moreover, the nature of the coordinated solvent also influences the SCM behaviour, with higher values of T_{max} for the series of $Co^{II}Cu^{II}$ chains with DMSO compared to those with H_2O, probably due to a better isolation of the chains because of the larger size of the former. At present, there are no reports on SCMs showing that the dynamics of magnetic relaxation is affected by interchain interactions, as our results suggest. Although the relevance of this unprecedented hypothesis must still be supported by new experimental and theoretical works, we guess that the implications that can be derived from it may be relevant to some of the proposed mechanisms for the slow magnetic relaxation of SCMs in the near future. We are currently exploring the limitations of this strategy by playing with the steric requirements of the substituents in the copper(II) precursor in order to obtain new members of this family of oxamato-bridged heterobimetallic SCMs with a higher blocking temperature.

Experimental Section

Reagents: Metal nitrates, sodium hydroxide, ethyl chlorooxoacetate and the corresponding aniline derivatives were purchased from commercial sources and used as received. Elemental analyses (C, H, N, S) were carried out by the Microanalytical Service of the Universitat de València.

***N*-2-methylphenyloxamate (H_2L^1), *N*-2,6-dimethylphenyloxamate (H_2L^2) and *N*-2,4,6-trimethylphenyloxamate (H_2L^3)**: The ethyl ester derivative of the proligands H_2L^x ($x=1$–3) were synthesised by following a standard procedure.[16] In a typical preparation, the corresponding aniline derivative (60 mmol) was treated with ethyl chlorooxoacetate (7.0 mL, 60 mmol) in THF (150 mL) at 0 °C under continuous stirring. The resulting solution was refluxed for 1 h and the solvent was removed on a rotatory evaporator to afford an oil which solidified when left at room temperature. The white solid obtained was filtered off, washed with a small amount of diethyl ether and dried under vacuum.

$Na_2[Cu(L^1)_2]\cdot 2H_2O$, $Na_2[Cu(L^2)_2]\cdot 2H_2O$ and $Na_2[Cu(L^3)_2]\cdot 6H_2O$: The sodium salts of the copper(II)–L^x (x = 1–3) precursors were prepared in a standardised manner.[16] In a typical experiment, the corresponding ethyl ester ligand derivative of H_2L^x (x = 1–3) (10 mmol) was suspended in water (25 mL) and allowed to react with an aqueous solution (25 mL) of NaOH (1.0 g, 25 mmol). A solution of $Cu(NO_3)_2\cdot 3H_2O$ (1.21 g, 5 mmol) in water (25 mL) was added dropwise to the resulting colourless solution at room temperature under continuous stirring. The resulting deep green solution was then filtered through paper to remove the small amount of solid particles. The solvent was reduced to one-fourth volume on a rotatory evaporator and a solid was formed. The green polycrystalline solid was filtered off, washed with acetone and diethyl ether and dried under vacuum. Well-formed prisms of $Na_2[Cu(L^3)_2]\cdot 6H_2O$ suitable for X-ray diffraction were obtained by slow diffusion of methanol into the aqueous mother liquor.

$[MnCu(L^1)_2]\cdot 2DMSO$ (1a), $[MnCu(L^2)_2]\cdot 2DMSO$ (2a) and $[MnCu(L^3)_2]\cdot 4DMSO$ (3a): Complexes **1a–3a** were prepared by the same synthetic procedure. In a typical experiment, $Mn(NO_3)_2\cdot 4H_2O$ (0.062 g, 0.25 mmol) was dissolved in hot DMSO (10 mL) (70 °C) and added dropwise to a solution of the corresponding sodium salt of the copper(II)–L^x (x = 1–3) precursor (0.25 mmol) dissolved in hot DMSO (10 mL). The resulting dark green solution was filtered while hot and the filtrate was allowed to stand at room temperature. After several days, a brownish green polycrystalline solid appeared which was collected by filtration and air-dried.

$[CoCu(L^1)_2]\cdot 3DMSO$ (1b), $[CoCu(L^2)_2]\cdot 3DMSO$ (2b) and $[CoCu(L^3)_2]\cdot 3DMSO$ (3b): Complexes **1b–3b** were prepared as indicated for **1a–3a** but with manganese(II) nitrate instead of cobalt(II) nitrate. In a typical experiment, $Co(NO_3)_2\cdot 6H_2O$ (0.073 g, 0.25 mmol) was dissolved in hot DMSO (10 mL) (70 °C) and added dropwise to a solution of the corresponding sodium salt of the copper(II)–L^x (x = 1–3) precursor (0.25 mmol) in hot DMSO (10 mL). The resulting dark green solution was filtered while hot, and the filtrate was allowed to stand at room temperature. After several days, a green polycrystalline solid appeared which was collected by filtration and air-dried.

$[CoCu(L^2)_2(H_2O)_2]$ (2b′) and $[CoCu(L^3)_2(H_2O)_2]\cdot 4H_2O$ (3b′): Well-formed deep green octahedral prisms of **2b′** and **3b′** suitable for X-ray diffraction were obtained by slow diffusion in an H-shaped tube of aqueous solutions containing stoichiometric amounts of the corresponding sodium salt of the copper(II)–L^x (x = 2 and 3) precursor (0.25 mmol) in one arm, and $Co(NO_3)_2\cdot 6H_2O$ (0.073 g, 0.25 mmol) in the other. They were isolated by filtration on paper and air-dried.

Physical techniques: ^1H NMR spectra were recorded at 250 MHz on a Bruker AC 250 spectrometer. Chemical shifts are reported in δ [ppm] versus $SiMe_4$ with the residual proton signals of deuterated DMSO solvent as internal standard. IR spectra were recorded on a Perkin-Elmer 882 spectrophotometer with KBr pellets. Variable-temperature dc and ac magnetic susceptibility measurements and variable-field magnetisation measurements were carried out on polycrystalline samples with a Quantum Design SQUID magnetometer. The susceptibility data were corrected for the diamagnetism of the constituent atoms and the sample holder.

X-ray crystal structure determination and refinement: The structures of $Na_2[Cu(L^3)_2]\cdot 6H_2O$, **2b′** and **3b′** were solved by direct methods and refined with full-matrix least-squares technique on F^2 using the SHELXS-97 and SHELXL-97 programs.[23a] Data collection and data reduction were done with the COLLECT[23b] and EVALCCD[23c] programs. Empirical absorption corrections were carried out using SADABS[23d] for all compounds. All calculations for data reduction, structure solution and refinement were done by standard procedures (WINGX).[23e] The final geometrical calculations and the graphical manipulations were carried out with PARST97[23f] and CRYSTAL MAKER[23g] programs, respectively. The hydrogen atoms of the organic ligands were calculated and refined with isotropic thermal parameters, while those from the water molecules were neither found nor calculated. Crystallographic data for $Na_2[Cu(L^3)_2]\cdot 6H_2O$, **2b′** and **3b′** are listed in Table S4 in the Supporting Information.

CCDC-611876 ($Na_2[Cu(L^3)_2]\cdot 6H_2O$), CCDC-611877 (**2b′**) and CCDC-227520 (**3b′**) contain the supplementary crystallographic data for this paper. These data can be obtained free of charge from the Cambridge Crystallographic Data Centre via www.ccdc.cam.ac.uk/data_request/cif.

Acknowledgements

This work was supported by the MEC (Projects CTQU2004-03633 and MAT2004-03112), the CNRS and the CAPES (Project COFECUB 460/04), the European Union through the Network QuEMolNa (Project MRTN-CT-2003-504880) and the Magmanet Network of Excellence (Contract 515767-2), the Generalitat Valenciana (Grupos 03/197) and the Gobierno Autónomo de Canarias (PI2002/175). E.P. and F.D. thank the Spanish Ministry of Science and Education for a grant.

[1] a) O. Kahn, *Molecular Magnetism*, VCH, New York, **1993**; b) O. Kahn, *Adv. Inorg. Chem.* **1995**, *43*, 179.

[2] a) A. Caneschi, D. Gatteschi, R. Sessoli, P. Rey, *Acc. Chem. Res.* **1989**, *22*, 392; b) A. Caneschi, D. Gatteschi, P. Rey, *Prog. Inorg. Chem.* **1991**, *39*, 331.

[3] a) O. Kahn, Y. Pei, M. Verdaguer, J. P. Renard, J. Sletten, *J. Am. Chem. Soc.* **1988**, *110*, 782; b) P. J. Van Kroningsbruggen, O. Kahn, K. Nakatani, Y. Pei, J. P. Renard, M. Drillon, P. Legoll, *Inorg. Chem.* **1990**, *29*, 3325; c) F. Lloret, K. Nakatani, Y. Journaux, O. Kahn, Y. Pei, J. P. Renard, *J. Chem. Soc. Chem. Commun.* **1988**, 642; d) K. Nakatani, J. Y. Carriat, Y. Journaux, O. Kahn, F. Lloret, J. P. Renard, Y. Pei, J. Sletten, M. Verdaguer, *J. Am. Chem. Soc.* **1989**, *111*, 5739; e) F. Lloret, M. Julve, R. Ruiz, Y. Journaux, K. Nakatani, O. Kahn, J. Sletten, *Inorg. Chem.* **1993**, *32*, 27.

[4] a) A. Caneschi, D. Gatteschi, J. P. Renard, P. Rey, R. Sessoli, *Inorg. Chem.* **1989**, *28*, 1976; b) A. Caneschi, D. Gatteschi, J. P. Renard, P. Rey, R. Sessoli, *Inorg. Chem.* **1989**, *28*, 2940; c) A. Caneschi, D. Gatteschi, J. P. Renard, P. Rey, R. Sessoli, *Inorg. Chem.* **1989**, *28*, 3314.

[5] a) A. Caneschi, D. Gatteschi, N. Lalioti, C. Sangregorio, R. Sessoli, G. Venturi, A. Vindigni, A. Rettori, M. G. Pini, M. Novak, *Angew. Chem.* **2001**, *113*, 1810; *Angew. Chem. Int. Ed.* **2001**, *40*, 1760; b) A. Caneschi, D. Gatteschi, N. Lalioti, R. Sessoli, L. Sorace, V. Tangoulis, A. Vindigni, *Chem. Eur. J.* **2002**, *8*, 286; c) A. Caneschi, D. Gatteschi, N. Lalioti, C. Sangregorio, R. Sessoli, G. Venturi, A. Vindigni, A. Rettori, M. G. Pini, M. Novak, *Europhys. Lett.* **2001**, *58*, 771; d) L. Bogani, A. Caneschi, M. Fedi, D. Gatteschi, M. Massi, M. A. Novak, M. G. Pini, A. Rettori, R. Sessoli, A. Vindigni, *Phys. Rev. Lett.* **2004**, *92*, 207204.

[6] R. Lescouëzec, L. M. Toma, J. Vaissermann, M. Verdaguer, F. S. Delgado, C. Ruiz-Perez, F. Lloret, M. Julve, *Coord. Chem. Rev.* **2005**, *249*, 2691.

[7] R. J. Glauber, *J. Math. Phys.* **1963**, *4*, 294.

[8] a) L. Thomas, F. Lionti, R. Ballou, D. Gatteschi, R. Sessoli, B. Barbara, *Nature* **1996**, *383*, 145; b) J. R. Friedman, M. P. Sarachik, J. Tejada, R. Ziolo, *Phys. Rev. Lett.* **1996**, *76*, 3830; c) C. Coulon, R. Clérac, L. Lecren, W. Wernsdorfer, H. Miyasaka, *Phys. Rev. B* **2004**, *69*, 132408.

[9] a) R. Clérac, H. Miyasaka, M. Yamashita, C. Coulon, *J. Am. Chem. Soc.* **2002**, *124*, 12837; b) H. Miyasaka, R. Clérac, K. Mizushima, K. Sugiura, M. Yamashita, W. Wernsdorfer, C. Coulon, *Inorg. Chem.* **2003**, *42*, 8203.

[10] a) R. Lescouëzec, J. Vaissermann, C. Ruiz-Pérez, F. Lloret, R. Carrasco, M. Julve, M. Verdaguer, Y. Dromzee, D. Gatteschi, W. Wernsdorfer, *Angew. Chem.* **2003**, *115*, 1521; *Angew. Chem. Int. Ed.* **2003**, *42*, 1483; b) L. M. Toma, R. Lescouëzec, F. Lloret, M. Julve, J. Vaissermann, M. Verdaguer, *Chem. Commun.* **2003**, 1850; c) L. M. Toma, R. Lescouëzec, J. Pasán, C. Ruiz-Pérez, J. Vaissermann, J. Cano, R. Carrasco, W. Wernsdorfer, F. Lloret, M. Julve, *J. Am. Chem. Soc.* **2006**, *128*, 4842.

[11] T. Liu, D. Fu, S. Gao, Y. Zhang, H. Sun, G. Su, Y. Liu, *J. Am. Chem. Soc.* **2003**, *125*, 13976.

[12] *S.* Wang, J. L. Zuo, *S.* Gao, Y. Song, H. C. Zhou, Y. Z. Zhang, X. Z. You, *J. Am. Chem. Soc.* **2004**, *126*, 8900.

[13] M. Ferbinteanu, H. Miyasaka, W. Wernsdorfer, K. Nakata, K. Sugiura, M. Yamashita, C. Coulon, R. Clérac, *J. Am. Chem. Soc.* **2005**, *127*, 3090.
[14] a) H. O. Stumpf, C. L. M. Pereira, A. C. Doriguetto, C. Konzen, L. C. B. Meira, N. G. Fernandes, Y. P. Mascarenhas, J. Ellena, M. Knobel, *Eur. J. Inorg. Chem.* **2005**, *24*, 5018; b) H. O. Stumpf, Y. Pei, L. Ouahab, F. Leberre, E. Codjovi, O. Kahn, *Inorg. Chem.* **1993**, *32*, 5687; c) H. O. Stumpf, Y. Pei, O. Kahn, J. Sletten, J. P. Renard, *J. Am. Chem. Soc.* **1993**, *115*, 6738.
[15] E. Pardo, R. Ruiz-García, F. Lloret, J. Faus, M. Julve, Y. Journaux, F. Delgado, C. Ruiz-Pérez, M. C. Muñoz, *Adv. Mater.* **2004**, *16*, 1597.
[16] B. Cervera, J. L. Sanz, M. J. Ibáñez, G. Villa, F. Lloret, M. Julve, R. Ruiz, X. Ottenwaelder, A. Aukauloo, S. Poussereau, Y. Journaux, M. C. Muñoz, *J. Chem. Soc. Dalton Trans.* **1998**, 781.
[17] a) J. M. Herrera, A. Bleuzen, Y. Dromzee, M. Julve, F. Lloret, M. Verdaguer, *Inorg. Chem.* **2003**, *42*, 7052; b) D. Maspoch, N. Domingo, D. Ruiz-Molina, K. Wurst, J. M. Hernández, G. Vaughan, C. Rovira, F. Lloret, J. Tejada, J. Veciana, *Chem. Commun.* **2005**, 5035.
[18] a) W. Wernsdorfer, N. Aliaga-Alcalde, D. N. Hendrickson, G. Christou, *Nature* **2002**, *416*, 406; b) W. Wernsdorfer, S. Bhaduri, R. Tiron, D. N. Hendrickson, G. Christou, *Phys. Rev. Lett.* **2002**, *89*, 197201; c) K. Park, M. R. Pederson, S. L. Richardson, N. Aliaga-Alcalde, G. Christou, *Phys. Rev. B* **2003**, *68*, 020405; d) S. Hill, R. S. Edwards, N. Aliaga-Alcalde, G. Christou, *Science* **2003**, *302*, 1015.
[19] a) R. Tiron, W. Wernsdorfer, N. Aliaga-Alcalde, G. Christou, *Phys. Rev. B* **2003**, *68*, 140407(R); b) R. Tiron, W. Wernsdorfer, D. Foguet-Albiol, N. Aliaga-Alcalde, G. Christou, *Phys. Rev. Lett.* **2003**, *91*, 227203; c) C. Boskovic, R. Bircher, P. L. W. Tregenna-Piggott, H. U. Güdel, C. Paulsen, W. Wernsdorfer, A. L. Barra, E. Khatsko, A. Neels, H. Stoeckli-Evans, *J. Am. Chem. Soc.* **2003**, *125*, 14046.
[20] a) H. Miyasaka, K. Nakata, K. Sugiura, M. Yamashita, R. Clérac, *Angew. Chem.* **2004**, *116*, 725; *Angew. Chem. Int. Ed.* **2004**, *43*, 707; b) J. Yoo, W. Wernsdorfer, E. C. Yang, M. Nakano, A. L. Rheingold, D. N. Hendrickson, *Inorg. Chem.* **2005**, *44*, 3377; c) H. Miyasaka, K. Nakata, L. Lecren, C. Coulon, Y. Nakazawa, T. Fujisaki, K. Sugiur, M. Yamashita, R. Clérac, *J. Am. Chem. Soc.* **2006**, *128*, 3770.
[21] a) K. S. Cole, R. H. Cole, *J. Chem. Phys.* **1941**, *9*, 341; b) C. J. F. Boettcher, *Theory of Electric Polarization*, Elsevier, Amsterdam, **1952**; c) S. M. Aubin, Z. Sun, L. Pardi, J. Krzysteck, K. Folting, L. J. Brunel, A. L. Rheingold, G. Christou, D. N. Hendrickson, *Inorg. Chem.* **1999**, *38*, 5329.
[22] a) M. A. Girtu, C. M. Wynn, W. Fujita, K. Awaga, A. Epstein, *J. Phys. Rev. B* **1998**, *57*, R11058; b) J. A. Mydosh, *Spin Glasses: An Experimental Introduction*, Taylor & Francis, London, **1993**; c) D. Chowdhury, *Spin Glasses and Other Frustrated Systems*, Princeton University Press, New Jersey, **1986**; d) K. Moorjani, J. M. Coey, *Magnetic Glasses*, Elsevier, New York, **1984**; e) K. Binder, A. P. Young, *Rev. Mod. Phys.* **1986**, *58*, 801.
[23] a) G. M. Sheldrick, SHELX97, Programs for Crystal Structure Analysis (Release 97-2), Universität Göttingen, Göttingen, Germany, **1998**; b) R. W. W. Hooft, COLLECT, Nonius BV, Delft, The Netherlands, **1999**; c) A. J. M. Duisenberg, L. M. J. Kroon-Batenburg, A. M. M. Schreurs, *J. Appl. Crystallogr.* **2003**, *36*, 220 (EVALCCD); d) SADABS, version 2.03, Bruker AXS Inc., Madison, WI, **2000**; e) L. J. Farrugia, *J. Appl. Cryst.* **1999**, *32*, 837; f) M. Nardelli, *J. Appl. Crystallogr.* **1995**, *28*, 659; g) D. Palmer, CRYSTAL MAKER, Cambridge University Technical Services, Cambridge, UK, **1996**.

Received: July 11, 2006
Published online: December 5, 2006

